Journal of Hazardous Materials 455 (2023) 131649

Contents lists available at ScienceDirect

Journal of Hazardous Materials

journal homepage: www.elsevier.com/locate/jhazmat

Research Article

An integrated characterisation of incineration bottom ashes towards sustainable application: Physicochemical, ecotoxicological, and mechanical properties

B.S. Bandarra [a,*,1], C. Mesquita [b], H. Passos [c], R.C. Martins [a], P.A.L.F. Coelho [b], J.L. Pereira [d], M. J. Quina [a]

[a] CIEPQPF, Department of Chemical Engineering, University of Coimbra, Rua Sílvio Lima, Pólo II-Pinhal de Marrocos, 3030-790 Coimbra, Portugal
[b] CITTA, Department of Civil Engineering, University of Coimbra, Rua Luís Reis Santos-Pólo II da Universidade, 3030-788 Coimbra, Portugal
[c] CICECO, Aveiro Institute of Materials, Department of Chemistry, University of Aveiro, 3810-193 Aveiro, Portugal
[d] CESAM, Centre for Environmental and Marine Studies, Department of Biology, University of Aveiro, 3810-193 Aveiro, Portugal

HIGHLIGHTS

- Leaching of bottom ashes was within safety benchmarks considered.
- No relevant ecotoxic effects were found for tested bottom ashes (impair < 22.7%).
- The battery of biotests used seems suitable for ecotoxicological assessment.
- Promising results were found for the mechanical properties of the materials.
- Potential for safe valorisation from an environmental and mechanical viewpoint.

GRAPHICAL ABSTRACT

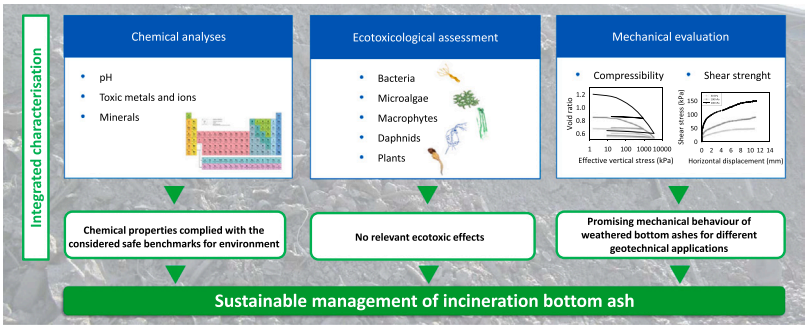

ARTICLE INFO

Editor: Edward Burton

Keywords:
IBA
Ecotoxicity
Biotests
Chemical composition
Geotechnical properties

ABSTRACT

Environmental protection is a central concern regarding municipal solid waste incineration bottom ash (IBA) management, but the assessment of waste Hazardous Property HP14 (ecotoxicity) is still under debate. Civil engineering applications may be a suitable management strategy. This work aimed at evaluating IBA regarding mechanical behaviour and environmental hazardous potential, including a biotest battery for ecotoxicity assessment (comprising miniaturised tests), to explore its potential for safe utilization. Physical, chemical, ecotoxicological (*Aliivibrio fischeri, Raphidocelis subcapitata, Lemna minor, Daphnia magna, Lepidium sativum*), and mechanical (one-dimensional compressibility, shear strength) analyses were performed. The low leaching for potentially toxic metals and ions complied with European Union (EU) limit values for non-hazardous waste landfills. No relevant ecotoxicological effects were found. The biotest battery seems suitable for ecotoxicological assessment in the aquatic ecosystem, providing wide information on waste impact on different trophic/functional levels and chemical uptake routes, simultaneously involving short-duration tests and reduced amounts of waste.

* Corresponding author.
E-mail addresses: bsbandarra@eq.uc.pt (B.S. Bandarra), carmenmesquita96@gmail.com (C. Mesquita), hpassos@ua.pt (H. Passos), martins@eq.uc.pt (R.C. Martins), pac@dec.uc.pt (P.A.L.F. Coelho), jpereira@ua.pt (J.L. Pereira), guida@eq.uc.pt (M.J. Quina).
[1] +351 239 798 700; +351 239 798 750

https://doi.org/10.1016/j.jhazmat.2023.131649
Received 3 February 2023; Received in revised form 9 May 2023; Accepted 14 May 2023
Available online 16 May 2023

IBA presented more compressibility than sand, but its mixture with sand (30%:70%) was closer to sand compressibility. IBA (lower stresses) and the mixture (higher stresses) showed slightly higher shear strength than sand. Overall, IBA presented the potential for valorisation as loose aggregates from an environmental and mechanical viewpoint in a circular economy framework.

1. Introduction

The management of municipal solid waste (MSW) plays an important role in sustainable development. An integrated approach is applied for MSW management in Europe, including incineration in waste-to-energy (WtE) plants. The WtE approach is widely adopted in developed countries since it produces energy, decreases waste volume (about 90%), diverts waste from landfills, treats non-recyclable waste, and keeps the material cycles clean (hygienization role and pollutants sink) [1,2]. The incineration process transforms organic materials mostly into CO_2 and H_2O, but the inorganic fraction remains as solid waste, including incineration bottom ash (IBA) and fly ash [1,3]. IBA accounts for nearly 80 wt% of incineration solid residues [4]. There are 463 operational MSW incineration plants in the European Union (EU), United Kingdom, Switzerland, and Norway that incinerate around 90 Mt/year of MSW and industrial waste of similar composition, resulting in 17.6 Mt/year of IBA [5]. The metallic fraction is usually recovered and used as secondary raw material in the metal industry [6]. However, the management practices addressing the mineral fraction are not consensual within Europe, with the percentage of utilisation (0–100 wt%) and the applications being diverse [5]. One of the major concerns driving discussion and constraining consensus has been the potential negative environmental impacts of IBA.

In this context, the assessment of the Hazardous Property HP 14 (“ecotoxic”) of waste defined in Commission Regulation (EU) No. 1357/2014 plays a key role in safeguarding environmental protection. Council Regulation (EU) 2017/997 provides a methodology for HP 14 assessment using calculation formulas and threshold values based on chemical composition of waste. However, Commission Decision 2014/955/EU states that results of experimental tests should prevail over calculation formulas, but there are no EU guidelines on experimental approaches for the HP 14 assessment. Although there is still no agreement on the methodology that should be followed, ecotoxicological tests have gained increasing recognition for the analyses of complex matrixes since these evaluate more realistically the environmental behaviour of waste by considering the effects of all components, interactions, and bioavailability [7–9]. Standardized tests with the bacteria *Aliivibrio fischeri*, the microalgae *Raphidocelis subcapitata,* and the microcrustacean *Daphnia magna* are frequently used for ecotoxicological assessment of chemicals and have been recommended for assessing waste [7]. These tests and the standardized test with *Lemna minor* (macrophyte) were previously used by the authors to evaluate the ecotoxicity of other inorganic waste [10,11]. In those studies, *Lemna minor* was found to be a useful test organism given that its systemic route of chemical uptake may add information to the surface contact uptake prevalent in microalgae, complementing ecotoxicological analysis covering producers in aquatic ecosystems. Moreover, germination tests may provide valuable knowledge on the phytotoxicity of waste, including IBA [12–17], and depending on the species used, the important and frequently disregarded interface between aquatic and soil compartments can be addressed in test batteries. Particularly, the miniaturised test (using the test plates from the Phytotoxkit [18]) with *Lepidium sativum* can be a valuable asset, while complying with practical principles such as low demand of waste and short test periods. Likewise, miniaturised tests of *R. subcapitata* and *L. minor* may be more practical and avoid the handling of greater amounts of waste and material in the laboratory. A few studies have analysed IBA but with different organisms and endpoints, and a broad range of responses was observed [12,15,19–21], which demonstrates the need of defining a methodology for HP 14 that can be robust to assess IBA in particular. The parallel analysis of the chemical composition is extremely relevant and should be complementary to biotests to better understand the potential environmental impacts. IBA is mainly formed of Si, Ca, Fe, Al, Na, and K minerals, exhibiting a composition similar to some geological materials [3]. Nevertheless, the chemical composition may differ according to particle size fractions, and the finest fraction usually has a higher concentration of potentially toxic metals (PTM), e.g., Cr, Cu, Cd, Ni, Pb, Zn, and chlorides [4,22–26] that can contribute to the leaching of those metals and salts [27,28].

The circular economy has been one of the main supporting pillars regarding waste management in the EU, as highlighted in waste legislation and more recently in the European Green Deal. Natural weathering of IBA by storing it outdoors for 6–20 weeks is the most frequent pre-treatment, leading to a more stable material [6,29]. The replacement of aggregates is one of the main potential applications for IBA given its geotechnical properties [30]. Indeed, IBA has the potential to be valorised as a secondary aggregate in civil engineering works, replacing natural aggregates like sand [6,30,31] e.g., in road-base, subbase, and embankments in road construction [5]. Other applications include its use in noise barriers, recovery in landfill sites, pipe bedding, filling, and restoration of degradable areas from extractive activities [1,5,6,30,32–34]. Still, the physical and mechanical properties of IBA must be analysed to evaluate their potential for safe use from a technical viewpoint if the aim is to apply these materials in civil engineering applications. In this context, compressibility and shear resistance provide a fundamental characterisation of the material as well as ecotoxicological assessment and chemical analysis that can be later combined with scale testing, which plays a key role when specific and defined applications are being considered [35–37], in order to evaluate the properties of materials in conditions closer to those of the real environment of the application. Limited data can be found in the literature regarding this characterisation of IBA, especially in the EU, where there is clearly a gap in this context [38–45]. Also, this evaluation of natural soils partially substituted by IBA is missing. This limits the valorisation of a material with a wide particle size distribution.

The proper valorisation of this material from a circular economy viewpoint allows the saving of natural resources and favours the decrease of IBA landfilling, hence mitigating the associated potential environmental impacts. Anchored in this arena, the present study aimed to assess the properties of weathered IBA regarding environmental and mechanical behaviour through an integrated and multidisciplinary assessment of its properties, analysing its potential for a safe application while evaluating the suitability of the assembled battery of biotests for HP 14 assessment. The mechanical properties of quartz sand were analysed for comparing IBA with a natural aggregate. A mixture of sand and IBA (70%:30%) was also assessed regarding mechanical properties to evaluate the effects of partially substituting sand with IBA. To the best of our knowledge, this study is the first to include such a holistic approach to IBA characterisation envisaging an environmentally safe and sustainable application.

2. Materials and methods

2.1. Materials

A sample of weathered IBA (aged more than 3 months) was provided by a WtE plant from Western Europe with a mass burning process operating above 1000 °C. The major input source of the incineration process is the unsorted domestic solid waste from households. In the WtE

plant, IBA from the furnace is cooled down through water quenching, and ferrous and non-ferrous metals are removed through magnetic separation and Eddy current, respectively. For weathering purposes, IBA is stored outdoors and exposed to ambient conditions in piles corresponding to monthly batches. The sample from this work was pooled from different sub-samples collected to cover the potential heterogeneity of an ageing pile (height and depth distribution considered). The sample was dried at room temperature (about 25 °C) and sieved through a sieve with a mesh size of 2 mm. This size fraction was chosen since higher concentrations of PTM are usually found in smaller particles of IBA [4,22–26] and due to size specifications in the mechanical tests performed. The material was then stored in a closed container until further testing. Representative subsamples were obtained for analyses using a sample splitter. Whenever necessary subsamples were crushed using a ball mill. Eluates were obtained from IBA for ecotoxicological testing and chemical composition analyses according to EN 12457–2. Thus, subsamples were agitated in an overhead shaker (Heidolph REAX 20) with distilled water at a liquid/solid (L/S) ratio of 10 L/kg for 24 h. The eluate was filtered using a 0.45 μm pore membrane. The concentration-response relationship in biotests was analysed by testing the organisms with different dilutions of this eluate. All test solutions were analysed with natural pH. Regarding the mechanical properties, quartz sand from Leiria (Portugal) was also analysed and used to prepare a mixture with IBA composed of 70% sand and 30% IBA (dry weight percentage), which was also characterised regarding those properties. Particles above 2 mm were also excluded in this case.

2.2. Physical and chemical characterisation

Based on the EPA Method 1684, IBA samples were dried at 105 °C for 24 h to determine moisture and afterwards calcinated at 550 °C for 2 h to calculate volatile solids (VS). VS were used as an estimation of the organic matter content in IBA. The density of solid particles (G) of IBA and sand was determined through pycnometry based on ASTM D854–14. The G of the mixture was estimated as the weighted average of measurements in IBA and sand. The particle size distribution of both materials (as received in the laboratory) was determined through sieving. For the mixture, the granulometry was obtained as the weighted average of IBA and sand. The coefficients of uniformity (C_U) and curvature (C_C) were calculated through Eqs. (1) and (2), as follows:

$$C_U = \frac{D_{60}}{D_{10}} \quad (1)$$

$$C_C = \frac{D_{30}^2}{D_{10} \times D_{60}} \quad (2)$$

Where: D_{60}, D_{30}, D_{10} – particle diameters below which 60%, 30%, and 10%wt of particles are found, respectively.

Electrical conductivity (EC) and pH were measured in the eluate obtained from IBA at L/S = 10 L/kg (EN 12457–2) using a multiparameter analyser (Consort C1020). The elemental composition of the eluate and the solid matrix of IBA was analysed through flame atomic absorption spectroscopy (FAAS) and total reflection x-ray fluorescence (TXRF). Analytikjena ContrAA 300 equipment (short-arc xenon lamp) and the Aspect CS 2.1.1.0 Tech:Flame software were used for FAAS. Microwave assisted acid digestion of the solid waste was performed with milled IBA (particle diameter < 0.075 mm) before FAAS to prepare samples according to the EPA Method 3051 A and using a TRANSFORM 680 Microwave Digestion System (Aurora Instruments). TXRF was performed using Bruker TXRF S2 PICOFOX equipment. Chlorides and sulphates were determined in IBA eluate through ion chromatography using Dionex ICS 5000+ equipment. Finally, the main crystalline phases of IBA powder (milled to < 0.075 mm) were identified through X-ray diffraction (XRD) using a PANalytical XPert PRO diffractometer (CuKα radiation, 2θ = 10–80°) with a graphite monochromator and the Panalytical High Score Plus 4.7 (PDF-4) software.

2.3. Ecotoxicological tests

Ecotoxicological assessment of freshly prepared IBA eluates was performed through a biotest battery (see Fig. S1 for a documentation of the apparatus) covering species from different trophic/functional levels in aquatic ecosystems: the bacteria *Aliivibrio fischeri*, representing decomposers; the microalgae *Raphidocelis subcapitata*, the macrophyte *Lemna minor*, and the garden cress *Lepidium sativum*, representing producers and covering different exposure routes; *Daphnia magna* representing primary consumers.

According to ISO 11348–2 for the *Aliivibrio fischeri* test, NaCl was added to eluates for osmotic adjustment and the test control was a 2% NaCl solution. Dr. Lange equipment and LUMIStox 300 software and kit were used, with bacteria being thawed immediately before the test. The luminescence inhibition was measured after 30 min of exposure to test solutions, and each treatment was tested in duplicate. The yield inhibition of *Raphidocelis subcapitata* was assessed based on cell density in triplicate. The methodology was based on OECD guideline 201 [46] adapted to 24-well microplates [47]. The microalgae inoculum was prepared with Woods Hole MBL culture medium [48] and adjusted to obtain an initial cell density of 10^4 cells/mL in each replicate, after microscopic cell counting in a Neubauer haemocytometer. Incubation occurred for 96 h under continuous illumination at 23 ± 1 ºC, and the final cell density was estimated from optical density measurements (440 nm) through a Shimadzu UV-1800 double-beam UV-Vis spectrophotometer. *Lemna minor* was cultured in Steinberg medium [49] and cultures were renewed once a week. Yield growth inhibition of *Lemna minor* considering frond number and dry weight was evaluated based on OECD guideline 221 [49] adapted to 6-well microplates [50]. The weight of three plants with three leaves was obtained after incubation at 60 °C for 24 h to determine the initial biomass. Nine fronds were tested per test replicate and three replicates were set per treatment. Incubation occurred for seven days under continuous illumination and at 23 ± 1 ºC as well, with the final number of fronds and the dry biomass being determined at the end of the test. The immobilisation of *Daphnia magna* was evaluated following OECD guideline 202 [51]. Monoclonal cultures were cultured in ASTM hard water medium [52] with an organic extract of *Ascophyllum nodosum* (macroalgae). Renewal of cultures occurred 3 times a week and *R. subcapitata* concentrated suspensions (3×10^5 cells/mL) were added as food. Neonates under 24 h old between the 3rd and 5th offspring were used for testing. Five organisms per replicate were tested and each treatment was tested in quadruplicate. The test was incubated for 48 h under 20 ± 2 ºC with a photoperiod of 16 h^L:8 h^D. The number of immobilised organisms was determined at the end of the test. The aforementioned tests are further detailed by the authors elsewhere [10,11].

In the *Lepidium sativum* test, artificial soil was prepared with 5% peat, 10% kaolinite clay, and 85% sand quartz according to ISO 18763 [50]. Test plates and filters from the Phytotoxkit [18] were used. Each test solution or distilled water (blank control) was mixed with 75 cm^3 of artificial soil and placed evenly in the lower compartment of the test plate. A paper filter was placed on the hydrated soil. After the filter was totally wet, 10 seeds were placed in one row at an equal distance from each other and around 1 cm from the middle ridge separating the two compartments of the test plate. Three replicates were tested for each solution. Test plates were incubated vertically in dark conditions at 25 ± 1 ºC for 72 h. Finally, each test plate was photographically documented to count the germinated seeds and measure the root lengths through the "Image J" image analysis programme [53]. Seed germination and root growth inhibitions were calculated according to ISO 18763.

Significant effects of IBA eluates were analysed through one-way ANOVA ($p < 0.05$). Then, Dunnett's test was used to compare IBA treatments with the control ($p < 0.05$) so that dilutions causing a

significant effect on test organisms could be identified. The nonparametric Kruskal-Wallis H test was carried out in cases where the Normality Test failed ($p < 0.05$) while heteroscedasticity did not fail in any dataset.

2.4. Geotechnical tests

2.4.1. Samples preparation

Mechanical testing of granular materials requires the use of suitable reconstituted samples. Because the use of IBA and its mixtures in this paper is not restricted to any particular application, all the samples were prepared using the dry pluviation method, which is one of the preferred methods to reconstitute granular materials, namely because the density can be properly controlled based only on the rate and height of pouring [54–56].

2.4.2. Analysis of compressibility using the oedometer test

One-dimensional compressibility was evaluated for sand, IBA, and the mixture (30% IBA:70% sand). Oedometer tests were performed to assess the variation of the void ratio with the vertical stress on the samples, using ASTM D2435–04 as a reference. The cylindrical samples tested (diameter = 70 mm; height = 19 mm) were subjected to vertical loads in the oedometer ring imposing the following sequence of vertical effective stress (σ'_v, in kPa): 1.5, 8.5, 16, 30, 58, 114, 226, 451, 901, 226, 58, 16, 58, 226, 901, 1801, 3600, 901, 226, 58, and 8.5. Load changes were made after settlements stabilization occurred. The initial dry unit weight (γ_d, in kN/m^3) and the initial void ratio (e_0) of each sample were determined through Eqs. (3) and (4), respectively:

$$\gamma_d = \frac{P_S}{V} \tag{3}$$

$$e_0 = \frac{G \times \gamma_w}{\gamma_d} - 1 \tag{4}$$

Where: P_S – dry weight of the sample (kN); V – volume occupied by the sample (m^3); G – density of solid particles; and γ_w – unit weight of water (= 9.81 kN/m^3).

The oedometers were connected to Linear Variable Differential Transformer (LVDT) transducers, measuring the vertical displacement (mm) over time for each load applied. Finally, the void ratio (e) (Eq. 5) per applied vertical stress (σ_v) was determined.

$$e = e_0 + \frac{\Delta h \times (1 + e_0)}{h_0} \tag{5}$$

Where: Δh – variation of the height of the sample in the oedometer ring (mm); h_0 – initial height of the sample in the ring (mm).

From the e-logσ'_v plots, the compression index (C_c) and the recompression index (C_r) were calculated as the slope of the virgin and recompression lines, respectively.

2.4.3. Analysis of shear strength using the direct shear test

Shear strength was analysed in the sand, IBA, and the mixture (30% IBA:70% sand) using the direct shear test to assess the shear resistance of the materials under different vertical (normal) effective stresses. This test is frequently used in road and backfill engineering to quickly evaluate the quality of the material backfill because of its effectiveness and convenience [41]. The shear box was 10 cm × 10 cm x 3.7 cm and tests were carried out with vertical effective stresses (σ_v') of 50 kPa, 100 kPa, and 200 kPa. The samples were sheared in dry conditions at a relatively low speed of 1.35 mm/min. The initial e_0 of samples was also determined according to Eq. (4). Two LVDT were coupled with the equipment allowing readings of the vertical and horizontal displacements of each sample during the test duration. The shear force applied in the horizontal plane of failure was measured by a dynamometric ring. Finally, the relationship between shear stress (τ) and horizontal displacement was plotted for different vertical stresses. The Mohr-Coulomb failure envelope was obtained based on the maximum shear stress and normal stress for each test, and subsequently, the cohesion (c') and the friction angle (Φ') of samples in terms of effective stresses were determined through a regression analysis to establish the Mohr-Coulomb failure envelope, described by Eq. (6). The vertical strain was calculated as the measured change in the height of the sample (Δh) normalized by the initial height (h_0).

$$\tau_f = c' + \sigma_f' \times tg(\Phi') \tag{6}$$

Where: τ_f – shear stress; σ'_f – normal effective stress; c' – cohesion; Φ' – friction angle; "f" and "'" denote *failure* and *effective stress conditions*, respectively.

3. Results and discussion

3.1. Chemical and physical characterisation

The initial weathered IBA sample presented a broad particle size distribution (Fig. 1), that was in line with other studies [34]. Adding IBA to sand in the mixture allowed extending the grain size distribution of both materials (Fig. 1). Based on the values of C_C and C_U calculated (Fig. 1) and following standard ASTM D 2487–85, the three materials studied were classified as well-graded sand (SW). Regarding solid particle density, G = 2.66 ± 0.02 was obtained for sand, agreeing with the accepted range for sand composed of quartz (2.65–2.67) [57]. A lower G of 2.36 ± 0.01 was obtained for IBA, within literature values (1.2–2.8) [34], which may favour its application e.g. in road embankments built over weaker foundation soils to reduce settlements, possibly replacing with environmental advantages other manufactured and recycled materials that have been used as lightweight fill for embankments [58–61]. Hereupon, a G of 2.57 was estimated for the mixture, which is close to the range expected for most soils (2.60–2.80) [62].

The experimental values obtained for the chemical properties of the solid matrix (Table 1) and eluates from IBA (Table 2) agreed with the literature. The natural pH of IBA (Table 2) was within the range for culture media used in the laboratory for the test organisms used and the range of tolerance for aquatic life (6.5–9) [63]. Regarding eluates, most PTM were below quantification limits for FAAS (Fe, Mn, Cd, Cr, Ni, Pb, and Zn; Table 2). The concentration of Zn complied with EU limit values for inert waste landfills according to Council Decision 2003/33/EC. The quantification limits for Cd, Cr, Ni, and Pb are above the limit values set for inert waste landfills, so it was not possible to confirm compliance with that criterion even though concentrations were very low. It should be noted, however, that Cd, Ni, and Pb are not expected in

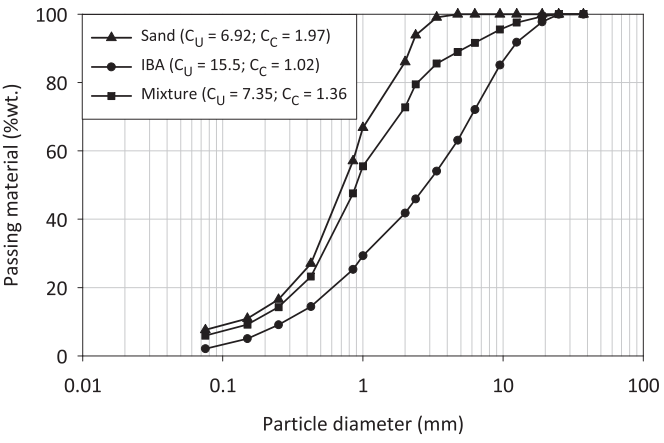

Fig. 1. Particle size distribution of IBA, sand, and the mixture (30% IBA:70% sand). Coefficients of uniformity (C_U) and curvature (C_C) are given between brackets.

Table 1
Chemical properties of IBA (dp < 2 mm) and literature values.

Parameter	IBA results	Literature
Moisture (%)	4.13 ± 0.06	7 – 30[c]
OM (%)	8.9 ± 0.1	0.2 – 12[d]
Elements (mg/kg)		
Ca	78,225 ± 4292[a]	56,300 – 306,429[e]
Na	12,176 ± 79[a]	11,352 – 57,723[e]
K	7980 ± 62[a]	6887 – 17,600[e]
Mg	9274 ± 133[a]	7080 – 30,660[e]
Fe	37,660 ± 28[a]	14,210 – 158,704[e]
P	4786 ± 756[b]	2401 – 24,014[e]
Ti	3227 ± 692[b]	2600 – 18,600[e]
Ba	348 ± 41[b]	400 – 3920[e]
Mn	396 ± 38[b]	83 – 3408[e]
Cd	< 3.6[a]	0.3 – 146[e]
Cu	894 ± 63[b]	190 – 12, 000[e]
Cr	109 ± 30[b]	21 – 3170[e]
Co	54 ± 5[b]	6 – 350[e]
Ni	65 ± 17[b]	7 – 4280[e]
Pb	508 ± 76[b]	98 – 13,700[e]
Sr	166 ± 26[b]	85 – 1000[e]
V	21 ± 2[b]	20 – 122[e]
Zn	3281 ± 91[a]	613 – 13,600[e]

[a] FAAS; [b] TXRF; [c] [33,34]; [d] [66,67]; [e] [3,21,24,68–84].

Table 2
Chemical properties of IBA (dp < 2 mm) eluate and literature values.

Parameter	IBA results	Literature	Limit value for inert waste landfill[h]	Limit value for non-hazardous waste landfill[h]
pH[a]	8.0 ± 0.2	8 – 10[e]	-	-
EC[a] (mS/cm)	2.72 ± 0.07	1.2 – 4[f]	-	-
Elements (mg/kg)				
Ca	4789 ± 25[c]	3000 – 9000[g]	-	-
Na	3671 ± 251[b]	1000 – 2500[g]	-	-
K	915 ± 142[b]	200 – 1000[g]	-	-
Mg	168 ± 5[b]	10 – 1000[g]	-	-
P	944 ± 259[c]	400 – 900[g]	-	-
Fe	< 0.8[b]	0.1 – 1[g]	-	-
Mn	< 0.23[b]	< 0.6[g]	-	-
Cd	< 0.18[b]	< 0.01 – 0.04[g]	0.04	1
Cu	5.2 ± 0.4[b]	0.20 – 8.22[g]	2	50
Cr	< 0.56[b]	0.05 – 1.40[g]	0.5	10
Ni	< 0.85[b]	< 0.03 – 0.15[g]	0.4	10
Pb	< 1.53[b]	0.03 – 0.5[g]	0.5	10
Zn	< 0.13[b]	0.04 – 1.7[g]	4	50
Ions (mg/kg)				
Cl^-	5474 ± 553[d]	1050 – 6700[g]	800	15,000
SO_4^{-2}	4306 ± 184[d]	288 – 9980[g]	1000	20,000

[a] L/S = 10 L/kg; [b] FAAS; [c] TXRF; [d] Ion chromatography; [e] Weathered IBA [29,85]; [f] Weathered IBA [3,86]; [g][1,3,21,29,69,73,87–90]; [h] Council Decision 2003/33/EC establishing criteria and procedures for the acceptance of waste at landfills.

concentrations above the limit values for inert landfills according to the literature and the quantification limit for Cr is close to the limit value established for this element (Table 2). As expected, based on the literature (Table 2), Cu was the PTM in higher concentration, exceeding those limit values. Nevertheless, all concentrations complied with EU limit values for non-hazardous waste landfills according to the same Regulation. It is noteworthy that although it may be toxic in higher concentrations, Cu is an essential metal with known biological functions e.g., cofactor of different enzymes [64,65]. Concentrations of chlorides (Cl^-) and sulphates (SO_4^{-2}) found also complied with limit values for non-hazardous landfill. It should be noted that leaching limit values for IBA utilisation in Europe are frequently above EU leaching limit values for inert waste landfill, and countries often consider the specific permitted application to establish those values [5].

Regarding mineral phases, the X-ray diffractogram (Fig. S2 in supplementary material) shows that IBA is mainly composed of quartz (SiO_2), which is in line with the literature [26,29,91]. Even though Si was not quantified due to technical limitations, other studies confirm that Si is indeed one of the main elements in IBA, typically in concentrations higher than 100 g/kg dry matter [69,83,84]. This is also the main mineralogical component of the sand from this study and one of the major constituents of the Earth's crust. Other common phases found included corundum (Al_2O_3), gehlenite ($Ca_2Al_2SiO_7$), and anorthite ($CaAl_2Si_2O_8$) [38,40,66,92–99]. Thus, the main mineral composition of IBA is similar to the mineral composition of natural and artificial aggregates [3,40,43,100].

3.2. Ecotoxicological assessment

Inhibitions below 50% were obtained for all analysed endpoints, and thus EC_{50} (median effect concentration) values could not be estimated for any of the tests. For *A. fischeri* (Fig. 2A), a maximum of 9.9% of bioluminescence inhibition was obtained for the undiluted eluate, and no significant differences between IBA treatments and the control were found ($H_6 = 9.564$; $p = 0.144$). These results are consistent with Ribé et al. [15], who did not find a full-breadth dose-response relationship and measured a maximum inhibition of 10% for an eluate concentration of 80% prepared from weathered IBA with pH 7.7–8.3. Römbke et al. [21] measured a maximum inhibition of 34.6% for the undiluted eluate of 1 out of 8 samples of weathered IBA with higher pH (8.7–12), and all the other 7 samples showed inhibitions below 14.3%. In the present study, all effects noticed were even below 20%. Fulladosa et al. [101] estimated the EC_{20} of several metals for *A. fischeri,* obtaining the following values: 0.46 ± 0.02 mg/L for Zn, 0.06 ± 0.02 mg/L for Pb, 0.26 ± 0.06 for Cu, 3.7 ± 0.33 mg/L for Cd, and 205 ± 6.30 mg/L for Cr. In our IBA eluates, Cu alone was found in concentrations above that EC_{20}. Nonetheless, it is important to highlight that IBA is a complex matrix, and interactions between substances play a role in ecotoxicity. Additionally, other components may contribute to stimulate bacteria biochemical reactions, overcoming other effects.

Regarding *R. subcapitata* (Fig. 2B), most yield inhibitions obtained were negative and the maximum inhibition determined was 10.7% (100% concentration), yet no significant inhibitory effects ($F_{6,\ 40} = 1.670$; $p = 0.158$) were confirmed. The negative values obtained indicate that test solutions favoured microalgae growth compared to control, which may be the result of beneficial additional nutrient load such as increased concentrations of K and P (Table 2). In Römbke et al. [21], 5 out of 8 weathered samples caused inhibitions below 30% for undiluted eluates. In fact, 4 of these samples were consistent with the results of the present study, leading to growth inhibitions below 13% and all of the 5 samples resulted in negative inhibitions for most concentrations. Stiernström et al. [102] prepared eluates from weathered IBA with 3 months (pH 10) and with more than 15 years (pH 6.8) through column leaching set to L/S = 10 L/kg, and no ecotoxicity was found in none of the samples neither through testing with *A. fischeri* nor *R. subcapitata*.

Growth inhibition of *Lemna minor* was below 20.9% (50% concentration) regarding the frond number (Figs. 2C) and 22.7% (6.25% concentration) concerning dry weight (Fig. 2D). IBA induced significant inhibitory effects regarding dry weight ($F_{6,\ 23} = 2.663$; $p < 0.001$), but

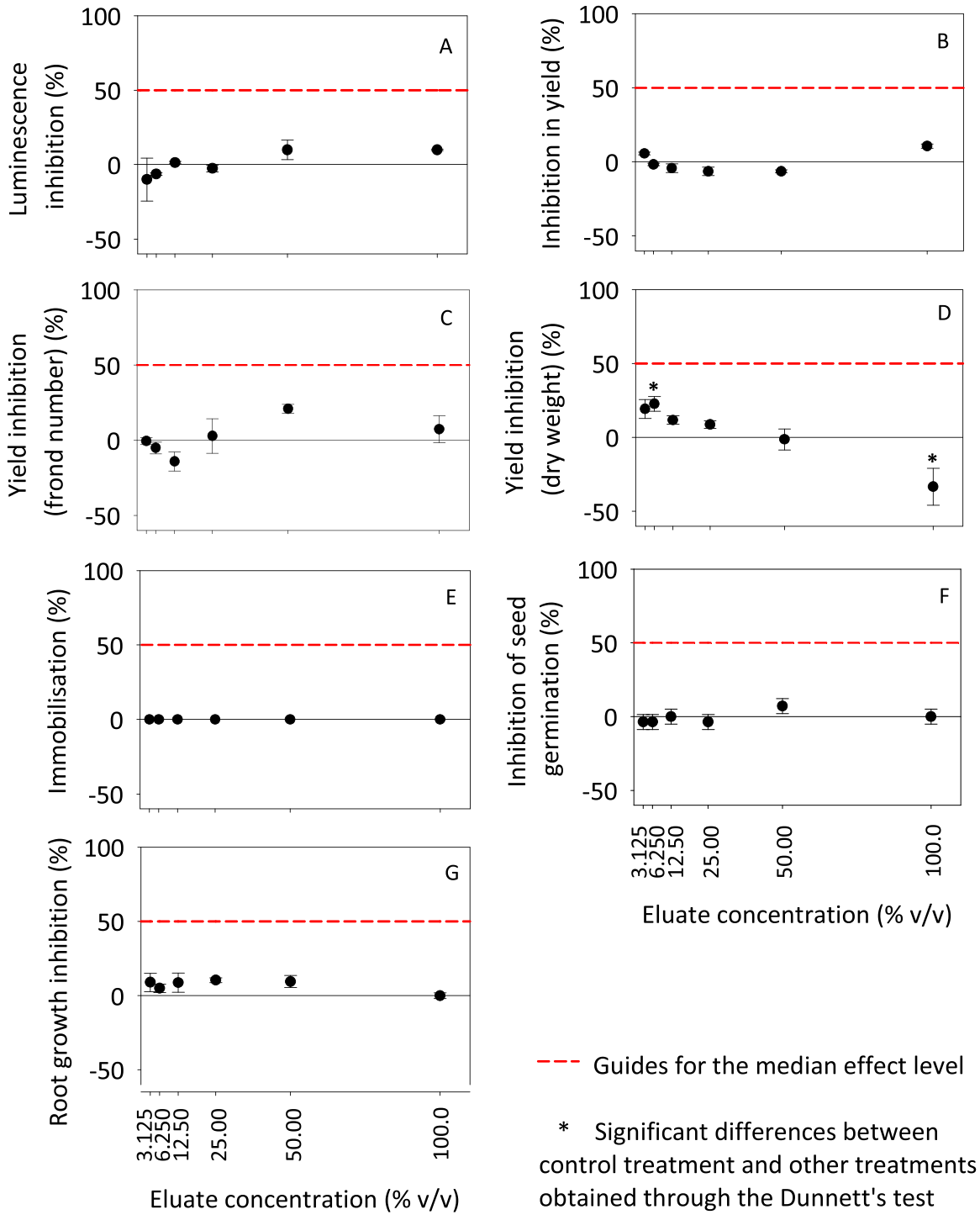

Fig. 2. Effects (mean ± standard error) of different concentrations (%v/v) of IBA eluate on test organisms: A) luminescence inhibition of *Aliivibrio fischeri*; B) inhibition in yield of *Raphidocelis subcapitata;* C) yield inhibition of *Lemna minor* considering frond number and D) dry weight*;* E) immobilisation of *Daphnia magna;* F) inhibition of seed germination and G) root growth inhibition of *Lepidium sativum*.

not regarding frond number ($F_{6,\ 23} = 8.903$; $p = 0.056$). Although no relevant ecotoxic effects were found, the dry weight seemed to be more sensitive to tested solutions than the frond number. As a strategy to cope with low contamination levels, plants may produce less biomass while maintaining frond growth as was the case in this study. This shows the need to evaluate both endpoints for a comprehensive assessment of waste ecotoxicity since they may not lead to the same conclusions. Even though neither microalgae nor *L. minor* displayed meaningful growth inhibitions, the negative impact in *L. minor* was slightly higher, possibly related to the complementary chemical uptake via systemic routes. The influence of having two chemical uptake routes was clearly observed in other studies [10,11] where waste eluates induced inhibitory effects in *L. minor* contrarily to what was observed for *R. subcapitata*, proving that the macrophytes can be a useful addition to ecotoxicological test batteries. In a European ring test on the ecotoxicological characterisation of waste [20], *L. minor* was tested with IBA eluates (pH = 10.42 ± 0.04), and 6 out of 10 tests resulted in $EC_{50} > 90\%$, indicating low ecotoxic effects. These contradictory results among studies focusing on IBA

eluates highlight the heterogeneity of these complex matrices and the consequent expectable variability in responses from indicator organisms.

In the test with *Daphnia magna*, no immobilisation was recorded for none of the test solutions with different concentrations of IBA eluate (Fig. 2E). Identical results were found by Römbke et al.[21] for 2 out of 8 samples of weathered IBA that presented no ecotoxicity. Nevertheless, the response to the 8 samples was widely variable and *D. magna* was the most sensitive aquatic organism compared to *A. fischeri* and *R. subcapitata*. In Lapa et al. [19], the sample with a pH closer to the sample of this study (pH = 8.9) did not induce ecotoxic effects in *D. magna*, and *R. subcapitata* was the most sensitive organism (EC_{50} = 25.7%). This variability in sensitivities highlights again the importance of running an ecotoxicological test battery including organisms from different trophic/functional levels rather than relying on a single indicator even for rapid screening. In Ribé et al. [15], *D. magna* was also the most sensitive organism and the authors indicate the relatively high concentration of Cr (1.28 ± 0.09 mg/L) and Cu (2.87 ± 0.29 mg/L) in the eluate as a possible explanation. Indeed, the concentrations in their study were well above the concentrations found in our IBA eluates (Table 2).

Finally, the response of *Lepidium sativum* to test solutions (Fig. 2F) was consistent with the remaining results. Indeed, the inhibition of seed germination was below 7% (50% concentration) and root growth inhibition was below 10% (50% concentration). No significant inhibitory effects were caused by exposure to IBA eluate regarding seed germination (H_6 = 5.867; p = 0.438) or regarding root growth ($F_{6,20}$ = 2.080, p = 0.121). Tintner et al. [14] tested solid fresh and artificially aged IBA with *L. sativum* and found a clear difference in results for fresh biomass and germination delay for the two types of materials: a decrease in biomass and an increase in germination delay were observed with increasing amounts of fresh IBA, while no effects were found for aged IBA except for the undiluted sample. Thus, this organism showed sensitivity to different samples. Aging (or weathering) leads to a more stable material with lower pH and bioavailability of PTM. Different pH was indeed observed for aged samples, and this may have contributed to the results obtained by Tintner et al. [14]. Bożym et al. [16] tested the leachate of a mineral-organic composite based on a mixture of sewage sludge and IBA. The leachate stimulated the growth of *L. sativum* seeds, and the authors attributed this to the low content of PTM and the presence of nitrogen compounds below toxic levels. Noteworthy is the comparatively lower concentration of Cu, Pb, and Zn found in the present study. IBA phytotoxicity has been studied with other species. For example, Phoungthong et al. [13] studied the effects of different conditions on leaching (extractant type, leaching time, L/S ratio, and leachate pH) on the phytotoxicity of IBA on wheat (*Triticum aestivum L.*) seed germination. The authors found that PTM concentrations in the leachate varied with pH and L/S ratio, but were less dependent on leaching time, highlighting the importance of establishing a leaching protocol. Leaching with distilled water resulted in low PTM concentrations, while other acid and alkaline extractants led to higher concentrations in leachates. Moreover, leaching at L/S = 10 L/kg for 24 h did not cause effects on seed germination.

Overall, the results above suggest that the sample of weathered IBA is not ecotoxic. As previously mentioned, weathering reduces pH as well as leaching potential, and both pH within the tolerance range for aquatic life and the low concentration of PTM in the eluate (also corroborated by the low EC of eluates; Table S1 in supplementary material) were likely favourable factors.

The assessment should be performed in different batches of IBA before any conclusion on the safety of the aimed downstream application due to recognized heterogeneity of this waste. It should be noted that fresh IBA or IBA subjected to other treatments may lead to different results regarding ecotoxicological assessment.

The limitations of the approach carried out are the ones inherent to the requirements that need to be met by laboratories that perform this type of analysis, such as the maintenance of cultures and adherence to the guidelines. Other limitations may arise as the discussion raises at the regulatory level, but at the moment testing with ecotoxicological models seems to bring more benefits than pitfalls to the rational and sustainable downstream application of waste.

3.3. Geotechnical evaluation

3.3.1. One-dimensional Compressibility

An elastoplastic behaviour was observed for all samples since deformations caused by the loading in the oedometer test were mostly irreversible (Fig. 3). The e-logσ'_v curves obtained for IBA, sand, and the mixture in the oedometer test (Fig. 3) present a smooth shape without the abrupt transitions in the void ratio typical of collapsible particles [103,104], suggesting that no significant particle crushing occur. The compression index (C_C) and the recompression index (C_r) were obtained for the three types of samples (Fig. 3). The C_r/C_c ratio for sand was around 1/7 and for IBA and the mixture was about 1/10, which is within the usual range for soils (1/10–1/5) [62] and is a good indication of the quality of the data.

The sand replicates did not show significant differences regarding *e*. The initial *e* (at σ'_v= 1.5 kPa*)* was found to be 0.67 ± 0.01 and the final *e* was 0.57 ± 0.01, at the highest stress applied (3600 kPa). The value obtained for the C_C of sand is within the range of 0.002–1 for the effective vertical stress range of 0.001–1000 MPa found in the literature [105]. Regarding C_r, values between 0.0023 and 0.0150 were found for sand by Zheng et al. [106] for maximum vertical stress of 300 kPa at dry conditions.

A different behaviour was shown by IBA since a much higher initial *e* was obtained (1.27 ± 0.09) and a large variation between initial and final *e* was found (*e* = 0.73 ± 0.09 for the maximum load). The higher initial *e* as well as the differences found between replicates result from the sample preparation method, which was designed to prepare samples of uniform sand and resulted in different values of *e* when applied to IBA samples. The value of C_c (0.405 ± 0.07) suggests that IBA is more compressible than sand. However, this difference is partly due to the significant differences in the initial *e,* IBA being in a much looser state. The fact that IBA is a very heterogeneous material regarding the

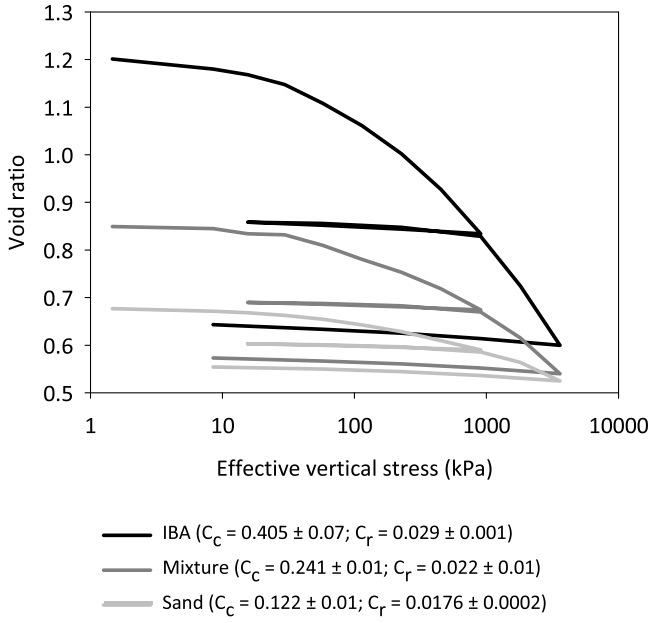

Fig. 3. Void ratio as a function of effective vertical stress (kPa) obtained in the oedometer test for the most representative sand, IBA, and mixture replicates. Compression (C_c) and recompression indexes (C_r) are given between brackets.

composition of particles, which have angular shape, contributed to these results. Becquart et al. [38] measured the one-dimensional compressibility of an uncompacted and dry sample of IBA using a maximum stress of 140 kPa, obtaining $C_c = 0.174 \pm 1.7 \times 10^{-4}$ and $C_r = 0.0019 \pm 3.2 \times 10^{-3}$. Considering that maximum stress, the C_c for IBA of this study would be 0.151 ± 0.01, indicating lower compressibility. In fact, stresses applied in this work provide a broad overview of compressibility behaviour, but such high stresses are seldom present in the kind of potential geotechnical applications for IBA that were earlier mentioned. In addition, the lower density of solid particles of IBA could also contribute to use it as filling material for embankments built on soft ground, where applied stresses would have to be necessarily low. Le et al. [40] also tested an uncompacted and dry sample with a maximum stress of 6613 kPa and obtained $C_c = 0.23$ and $C_s = 0.0062$. C_s is the swelling index (slope of the swelling line in the unloading curve) and its value is approximately the value of C_r. In the aforementioned study, the initial *e* was significantly lower (around 0.95), which may explain the lower compressibility of that sample. The compressibility of samples can be

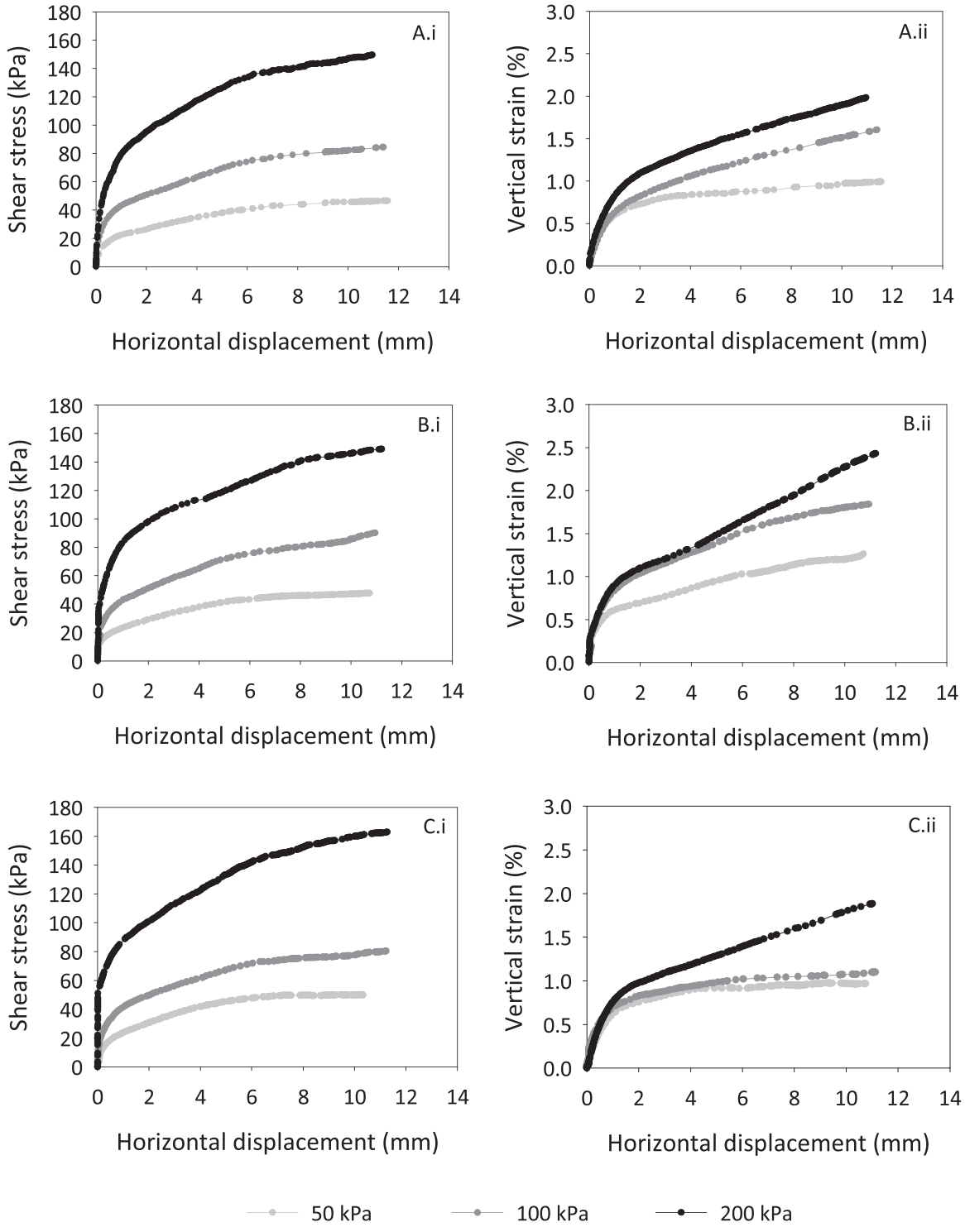

Fig. 4. Shear stress (i) and vertical strain (ii) as a function of horizontal displacement for sand (A), IBA (B), and the mixture (C).

reduced with compaction if needed in view of the specific application considered for IBA.

Generally, good reproducibility was obtained for the mixture with the sample preparation method in this study. The initial *e* increased compared to sand to 0.85 ± 5.6 × 10^{-4}. A less evident small increase was also found regarding *e* for the higher stress (*e* = 0.60 ± 0.02). Hence, the mixture shows a behaviour closer to the sand. The value of C_c obtained for the mixture shows that it was less compressible than IBA but more compressible than sand. However, these results are clearly affected by the differences in the initial void ratio of the samples. These properties would be suitable for applications such as filling material in noise barriers and degradable areas from extractive activities for restoration. For other applications, such as road embankments, compaction of these materials should result in a reduction of compressibility.

3.3.2. Shear strength

The sample preparation method resulted in initial void ratios qualitatively similar to those obtained in the oedometer, with average and standard deviations of 0.66 ± 0.02 for sand, 1.28 ± 0.11 for IBA, and 0.69 ± 0.08 for the mixture.

For each test, the shear stress (τ) increased with increasing horizontal displacement until stabilization when the material reached its τ_{max} (Fig. 4 A.i, B.i, Ci). This behaviour is expected for loose aggregates and reflects the fairly loose condition of all the samples tested. The Figures representing the τ_{max} as a function of σ'_v resulted in a linear regression with a high degree of correlation above 0.99 (Fig. 5), from which the shear strength parameters (c' and Φ') were determined (Table 3).

The low values of c', which should be around zero in non-cemented granular materials [107], possibly reflect the non-linearity of the failure envelope for lower stress levels. The fact that the c' value of IBA is slightly higher may result from the presence of elongated particles crossing the horizontal shear plane, thus increasing the shear resistance at low normal stresses. The friction angle of the samples from this study is coherent with the typical range for well-graded sand (33–45°) [108]. Gupta et al. [39] found Φ'= 43.3–49.7 for a sample of IBA tested in comparable conditions. Similarly, Muhunthan et al. [44] tested a sample under normal stresses of 5.5, 11, and 16.2 kPa and obtained c' (9.6 kPa) and Φ' (50.2°) values that are slightly lower and higher, respectively, than the values in this work for IBA. These divergences are possibly due to the fact that samples from those studies were compacted before the test. Three materials presented good and similar shear strength (Fig. 5). Nonetheless, both IBA, for lower effective stress (< 50 kPa), and the mixture, for greater effective stress, revealed slightly higher shear strengths than sand. This may result from the larger grain size distribution of these materials and the larger angularity of IBA particles. Thus,

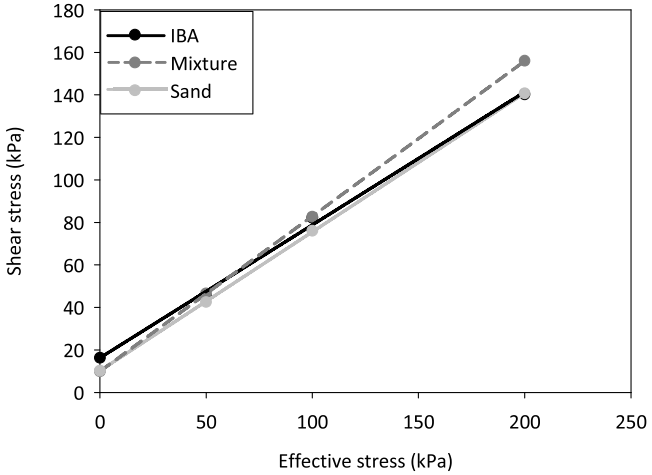

Fig. 5. Mohr-Coulomb failure envelope for sand, IBA, and the mixture.

Table 3
Shear strength properties of each material obtained from the shear box test.

Sample	σ_v' (kPa)	τ_{max} (kPa)	c' (kPa)	Φ' (°)
Sand	50	42.5 ± 3.5	10.2	33.2
	100	76.0 ± 0.1		
	200	140.1 ± 4.8		
IBA	50	45.3 ± 1.2	16.2	32.0
	100	82.2 ± 0.07		
	200	140.2 ± 4.3		
Mixture	50	46.6 ± 4.4	9.9	36.1
	100	82.7 ± 7.6		
	200	156.0 ± 1.5		

IBA showed good potential for utilization both alone and in mixtures with granular materials from a shear strength perspective.

Based on the vertical strain variation with the horizontal displacement for sand, IBA, and the mixture (Fig. 4 A.ii, B.ii, C.ii), all materials demonstrated a behaviour similar to loose sand for all applied normal stresses. In fact, constant contraction was observed for all samples throughout the test, which is a good indication of the quality of the tests considering the loose condition of the tested samples. IBA seemed to be the one contracting the most during shear, due to the highest initial void ratio.

4. Conclusions

Weathered IBA, well-graded sand, and a mixture (30% IBA:70% sand) were characterised and compared. From the physical viewpoint, IBA and the mixture are similar to well-graded sand regarding particle size distribution. The solid particle density of the mixture was close to the typical range for soils, while IBA exhibited lower density. The main mineral composition of IBA is similar to natural and synthetic aggregates. IBA presented low leaching potential, complying with EU limit values for non-hazardous waste landfills regarding PTM and ions analysed. The ecotoxicological evaluation was consistent with the chemical results since no relevant ecotoxic effects were found in any of the 5 biotests. Indeed, the results are within the natural biological variability and the maximum inhibition found was 22.7% (*L. minor* biomass yield). This test in particular can provide information on plant-related ecotoxicity, but the evaluation of different samples of IBA with this organism is lacking in the literature. The biotest battery seems not only suitable (includes representative species from different trophic/functional levels and chemical uptake pathways) but also practical since miniaturised tests involve the handling of reduced amounts of waste and material in the laboratory. HP 14 regulatory framework needs to be revised promoting proper environmental protection, while allowing the efficient valorisation of non-hazardous waste. Further research is needed to support the establishment of the most suitable ecotoxicological testing approaches for similar types of waste, namely regarding test organisms, endpoints, and methodologies at the regulatory level in the EU. These should focus on efficient (cost- and time-efficient, thus economically sustainable also from the producing industry perspective) standard ecotoxicological test batteries. The natural pH 8 of IBA eluates within the tolerance range for aquatic life contributed to avoiding pH-related deleterious effects. Moreover, the low concentration of PTM in eluates was probably another beneficial factor. In summary, the weathered IBA from this study is not ecotoxic, opening the possibility for valorisation from an environmental viewpoint. Regarding mechanical properties, IBA apparently presented more compressibility than sand, mostly because IBA samples were initially looser. When considering specific applications, compacting the samples would lead to different conclusions since samples showed similar qualitative behaviour. Furthermore, IBA is much less compressible for lower stress. These results and the lower density of solid particles might favour its use in embankments built on softer soils. The compressibility of the mixture was much closer to sand. On the other hand, a slightly higher shear

strength was found both for IBA (for lower effective stress) and the mixture (for higher effective stress) when compared to sand, even if these samples were tested in a looser condition, which may be due to the presence of angular particles and a better interlocking resulting from the wider grain size distribution. Thus, weathered IBA displayed promising results regarding mechanical properties, mixed or not with granular materials. Globally, IBA from this study showed potential for valorisation both from environmental and mechanical viewpoints. Possible applications include its use in noise barriers, restoration of areas of extractive activities, drains, pipe bedding, and road embankments, especially when built on soft ground (the latter needing relevant amounts of materials). Future research should include the evaluation of different mixtures (proportions and types of soils) and sample preparation methods that truly simulate a specific application to better evaluate the promising potential of IBA for different geotechnical applications in a circular economy framework, contributing to avoiding landfilling and unnecessary exploitation of natural resources. From this study, interesting results were obtained with IBA collected from one batch of one WtE plant to analyse IBA potential for application regarding mechanical properties as well as to contribute towards broad evaluation of the suitability of a battery of biotests for waste assessment for further analysis of IBA potential for application regarding environmental impacts. Nonetheless, it is important to bear in mind that different batches must be evaluated for a specific application of the material due to its heterogeneity. It should be also mentioned that scale testing may play a key role when specific and defined applications are being considered in order to evaluate the properties of materials in conditions closer to those of the real environment of the application.

Environmental Implication

European List of Waste classifies municipal solid waste incineration bottom ash (IBA) as mirror entry: codes 19 01 11* (bottom ash and slag containing hazardous substances) or 19 01 12 (bottom ash and slag other than those mentioned in 19 01 11). IBA must be evaluated for reliable classification. This is challenging given its great heterogeneity in composition and particle size, possibly containing high concentrations of potentially toxic metals. The work aims at evaluating environmental hazardous potential through chemical analyses and assessment of a biotest battery for waste ecotoxicity, simultaneously evaluating mechanical properties envisaging potential environmentally safe management considering circular economy.

CRediT authorship contribution statement

B.S. Bandarra: Conceptualization, Methodology, Validation, Formal analysis, Investigation, Data curation, Writing – original draft, Visualisation. **C. Mesquita:** Investigation, Writing – review & editing. **H. Passos:** Investigation, Resources, Writing – review & editing. **R.C. Martins:** Conceptualization, Resources, Writing – review & editing, Supervision. **P.A.L.F. Coelho:** Conceptualization, Methodology, Resources, Writing – review & editing, Supervision. **J.L. Pereira:** Conceptualization, Methodology, Resources, Writing – review & editing, Supervision. **M.J. Quina:** Conceptualization, Resources, Writing – review & editing, Supervision.

Declaration of Competing Interest

The authors declare that they have no known competing financial interests or personal relationships that could have appeared to influence the work reported in this paper.

Data Availability

The authors are unable or have chosen not to specify which data has been used.

Acknowledgments

Thanks are due to FCT/MCTES for their financial support to CIEPQPF (UIDB/00102/2020), CESAM (UIDP/50017/2020 + UIDB/50017/2020 + LA/P/0094/2020), and CICECO (UIDB/50011/2020, UIDP/50011/2020 & LA/P/0006/2020) through national funds. B.S.B. is the recipient of an individual research grant by the FCT/MCTES with the reference SFRH/BD/147920/2019, through national funds and ESF (European Social Fund). H. Passos acknowledges FCT – Fundação para a Ciência e a Tecnologia, I.P. for the researcher contract CEECIND/00831/2017 under the Scientific Employment Stimulus - Individual Call 2017.

Appendix A. Supporting information

Supplementary data associated with this article can be found in the online version at doi:10.1016/j.jhazmat.2023.131649.

References

[1] Bandarra, B.S., Pereira, J.L., Martins, R.C., Maldonado-Alameda, A., Chimenos, J. M., Quina, M.J., 2021. Opportunities and barriers for valorizing waste incineration bottom ash: Iberian countries as a case study. Appl Sci 11, 9690. https://doi.org/10.3390/app11209690.

[2] Bandarra, B.S.; Quina, M.J. Municipal Solid Waste Incineration and Sustainable Development. In Advances in Sustainable Energy: Policy, Materials and Devices; Gao, Y.-J., Song, W., Liu, J.L., Bashir, S., Eds.; Springer, 2021 ISBN 9783030744052.

[3] Forteza, R., Far, M., Seguí, C., Cerdá, V., 2004. Characterization of bottom ash in municipal solid waste incinerators for its use in road base. Waste Manag 24, 899–909. https://doi.org/10.1016/j.wasman.2004.07.004.

[4] Chimenos, J.M., Segarra, M., Fernández, M.A., Espiell, F., 1999. Characterization of the bottom ash in municipal solid waste incinerator. J Hazard Mater 64, 211–222. https://doi.org/10.1016/S0304-3894(98)00246-5.

[5] Blasenbauer, D., Huber, F., Lederer, J., Quina, M.J., Blanc-Biscarat, D., Bogush, A., Bontempi, E., Blondeau, J., Chimenos, J.M., Dahlbo, H., et al., 2020. Legal situation and current practice of waste incineration bottom ash utilisation in Europe. Waste Manag 102, 868–883. https://doi.org/10.1016/j.wasman.2019.11.031.

[6] CEWEP - Confederation of European Waste-to-Energy Plants. Bottom Ash Factsheet. Available online: http://www.cewep.eu/2017/09/08/bottom-ash-factsheet/ (accessed on Mar 11, 2020).

[7] Pandard, P., Römbke, J., 2013. Proposal for a "harmonized" strategy for the assessment of the HP 14 property. Integr Environ Assess Manag 9, 665–672. https://doi.org/10.1002/ieam.1447.

[8] Bandarra, B.S., Silva, S., Pereira, J.L., Martins, R.C., Quina, M.J., 2022. A study on the classification of a mirror entry in the European list of waste: incineration bottom ash from municipal solid waste. Sustainability 14, 10352. https://doi.org/10.3390/su141610352.

[9] Wilke, B.M., Riepert, F., Koch, C., Kühne, T., 2008. Ecotoxicological characterization of hazardous wastes. Ecotoxicol Environ Saf 70, 283–293. https://doi.org/10.1016/j.ecoenv.2007.10.003.

[10] Bandarra, B.S., Gomes, L.A., Pereira, J.L., Gonçalves, F.J.M., Martins, R.C., Quina, M.J., 2019. Characterization of ecotoxicological effects of green liquor dregs from the pulp and paper industry. ACS Sustain Chem Eng 7, 14707–14715. https://doi.org/10.1021/acssuschemeng.9b02636.

[11] Bandarra, B.S., Gomes, L.A., Pereira, J.L., Gonçalves, F.J.M., Martins, R.C., Quina, M.J., 2020. Assessment of hazardous property HP 14 using ecotoxicological tests: a case study of weathered coal fly ash. Environ Sci Pollut Res 27, 20972–20983. https://doi.org/10.1007/s11356-020-08515-8.

[12] Ferrari, B., Radetski, C.M., Veber, A.M., Ferard, J.F., 1999. Ecotoxicological assessment of solid wastes: a combined liquid- and solid-phase testing approach using a battery of bioassays and biomarkers. Environ Toxicol Chem 18, 1195–1202. https://doi.org/10.1897/1551-5028(1999)018<1195:EAOSWA>2.3.CO;2.

[13] Phoungthong, K., Zhang, H., Shao, L.M., He, P.J., 2016. Variation of the phytotoxicity of municipal solid waste incinerator bottom ash on wheat (Triticum aestivum L.) seed germination with leaching conditions. Chemosphere 146, 547–554. https://doi.org/10.1016/j.chemosphere.2015.12.063.

[14] Tintner, J., Matiasch, L., Klug, B., 2016. Germination and juvenile development of plants on municipal solid waste incineration (MSWI) slag. Ecol Eng 87, 162–167. https://doi.org/10.1016/j.ecoleng.2015.11.037.

[15] Ribé, V., Nehrenheim, E., Odlare, M., 2014. Assessment of mobility and bioavailability of contaminants in MSW incineration ash with aquatic and terrestrial bioassays. Waste Manag 34, 1871–1876. https://doi.org/10.1016/j.wasman.2013.12.024.

[16] Bożym, M., Król, A., Mizserna, K., 2021. Leachate and contact test with Lepidium sativum L. to assess the phytotoxicity of waste. Int J Environ Sci Technol 18, 1975–1990. https://doi.org/10.1007/s13762-020-02980-x.

[17] Mierzwa-Hersztek, M., Krzysztof, G., Marcin, J., Krzysztof, D., 2019. Assessment of energy parameters of biomass and biochars, leachability of heavy metals and

phytotoxicity of their ashes. J Mater Cycles Waste Manag 21, 786–800. https://doi.org/10.1007/s10163-019-00832-6.
[18] MicroBioTests Inc. Phytotoxkit Standard Operational Procedure. 2005.
[19] Lapa, N., Barbosa, R., Morais, J., Mendes, B., Méhu, J., Santos Oliveira, J.F., 2002. Ecotoxicological assessment of leachates from MSWI bottom ashes. Waste Manag 22, 583–593. https://doi.org/10.1016/S0956-053X(02)00009-0.
[20] Moser, H.; Römbke, J. Ecotoxicological characterization of waste - Results and experiences of a European ring test; Springer Ltd.: New York, USA, 2009; ISBN 9780387889580.
[21] Römbke, J., Moser, T., Moser, H., 2009. Ecotoxicological characterisation of 12 incineration ashes using 6 laboratory tests. Waste Manag 29, 2475–2482. https://doi.org/10.1016/j.wasman.2009.03.032.
[22] Chen, C.H., Chiou, I.J., 2007. Distribution of chloride ion in MSWI bottom ash and de-chlorination performance. J Hazard Mater 148, 346–352. https://doi.org/10.1016/j.jhazmat.2007.02.046.
[23] Xia, Y., He, P., Shao, L., Zhang, H., 2017. Metal distribution characteristic of MSWI bottom ash in view of metal recovery. J Environ Sci 52, 178–189. https://doi.org/10.1016/j.jes.2016.04.016.
[24] Tang, J., Steenari, B.M., 2016. Leaching optimization of municipal solid waste incineration ash for resource recovery: a case study of Cu, Zn, Pb and Cd. Waste Manag 48, 315–322. https://doi.org/10.1016/j.wasman.2015.10.003.
[25] Luo, H., Cheng, Y., He, D., Yang, E.H., 2019. Review of leaching behavior of municipal solid waste incineration (MSWI) ash. Sci Total Environ 668, 90–103. https://doi.org/10.1016/j.scitotenv.2019.03.004.
[26] Alam, Q., Schollbach, K., Hoek, C., Van, Laan, Van Der, S., Wolf, T., De; Brouwers, H.J.H., 2019. In-depth mineralogical quantification of MSWI bottom ash phases and their association with potentially toxic elements. Waste Manag 87, 1–12. https://doi.org/10.1016/j.wasman.2019.01.031.
[27] Van Der Sloot, H.A., Kosson, D.S., Hjelmar, O., 2001. Characteristics, treatment and utilization of residues from municipal waste incineration. Waste Manag 21, 753–765. https://doi.org/10.1016/S0956-053X(01)00009-5.
[28] Weibel, G., Eggenberger, U., Kulik, D.A., Hummel, W., Schlumberger, S., Klink, W., Fisch, M., Mäder, U.K., 2018. Extraction of heavy metals from MSWI fly ash using hydrochloric acid and sodium chloride solution. Waste Manag 76, 457–471. https://doi.org/10.1016/j.wasman.2018.03.022.
[29] Maldonado-Alameda, À., Giro-Paloma, J., Alfocea-Roig, A., Formosa, J., Chimenos, J.M., 2020. Municipal solid waste incineration bottom ash as sole precursor in the alkali-activated binder formulation. Appl Sci 10, 4129. https://doi.org/10.3390/APP10124129.
[30] Dou, X., Ren, F., Nguyen, M.Q., Ahamed, A., Yin, K., Chan, W.P., Chang, V.W.C., 2017. Review of MSWI bottom ash utilization from perspectives of collective characterization, treatment and existing application. Renew Sustain Energy Rev 79, 24–38. https://doi.org/10.1016/j.rser.2017.05.044.
[31] Van Praagh, M., Johansson, M., Fagerqvist, J., Grönholm, R., Hansson, N., Svensson, H., 2018. Recycling of MSWI-bottom ash in paved constructions in Sweden – a risk assessment. Waste Manag 79, 428–434. https://doi.org/10.1016/j.wasman.2018.07.025.
[32] Born, J.-P.; Van Brecht, A. Recycling potentials of MSWI Bottom Ash Available online: https://www.cewep.eu/wp-content/uploads/2017/10/1318_avb_and_jp_born_2014_cewep_conference_bottom_ash_reuse.pdf (accessed on Jan 27, 2022).
[33] Joseph, A.M., Snellings, R., Van den Heede, P., Matthys, S., De Belie, N., 2018. The use of municipal solid waste incineration ash in various building materials: a Belgian point of view. Mater (Basel) 11. https://doi.org/10.3390/ma11010141.
[34] Lynn, C.J., Ghataora, G.S., Dhir, OBE, R.K., 2017. Municipal incinerated bottom ash (MIBA) characteristics and potential for use in road pavements. Int J Pavement Res Technol 10, 185–201. https://doi.org/10.1016/j.ijprt.2016.12.003.
[35] Yin, K., Chan, W.P., Dou, X., Lisak, G., Wei-Chung Chang, V., 2020. Comparison and modeling of leachate transportation dominated by the field permeability with an anisotropic characteristic based on a large-scale field trial study. Chemosphere 242, 125254. https://doi.org/10.1016/j.chemosphere.2019.125254.
[36] Chan, W.P., Ren, F., Dou, X., Yin, K., Chang, V.W.C., 2018. A large-scale field trial experiment to derive effective release of heavy metals from incineration bottom ashes during construction in land reclamation. Sci Total Environ 637–638, 182–190. https://doi.org/10.1016/j.scitotenv.2018.05.026.
[37] Spreadbury, C.J., McVay, M., Laux, S.J., Townsend, T.G., 2021. A field-scale evaluation of municipal solid waste incineration bottom ash as a road base material: Considerations for reuse practices. Resour Conserv Recycl 168, 105264. https://doi.org/10.1016/j.resconrec.2020.105264.
[38] Becquart, F., Bernard, F., Edine, N., Zentar, R., 2009. Monotonic aspects of the mechanical behaviour of bottom ash from municipal solid waste incineration and its potential use for road construction. Waste Manag 29, 1320–1329. https://doi.org/10.1016/j.wasman.2008.08.019.
[39] Gupta, G., Datta, M., Ramana, G.V., Alappat, B.J., 2021. MSW incineration bottom ash (MIBA) as a substitute to conventional materials in geotechnical applications: a characterization study from India and comparison with literature. Constr Build Mater 308, 124925. https://doi.org/10.1016/j.conbuildmat.2021.124925.
[40] Le, H.N., Razakamanantsoa, A., Nguyen, M., Phan, V.T., Dao, P., Nguyen, D.H., 2018. Evaluation of physicochemical and hydromechanical properties of MSWI bottom ash for road construction. Waste Manag 80, 168–174. https://doi.org/10.1016/j.wasman.2018.09.007.
[41] Lin, C.-L., Weng, M.-C., Chang, C.-H., 2012. Effect of incinerator bottom-ash composition on the mechanical behavior of backfill material. J Environ Manag 113, 377–382. https://doi.org/10.1016/j.jenvman.2012.09.013.
[42] Huang, Y., Chen, J., Shi, S., Li, B., Mo, J., Tang, Q., 2020. Mechanical properties of municipal solid waste incinerator (MSWI) bottom ash as alternatives of subgrade materials. Adv Civ Eng 1–11.
[43] Xie, R., Xu, Y., Huang, M., Zhu, H., Chu, F., 2017. Assessment of municipal solid waste incineration bottom ash as a potential road material. Road Mater Pavement Des ISSN 18, 992–998. https://doi.org/10.1080/14680629.2016.1206483.
[44] Muhunthan, B., Taha, R., Said, J., 2004. Geotechnical engineering properties of incinerator ash mixes. J Air Waste Manag Assoc 54, 985–991. https://doi.org/10.1080/10473289.2004.10470959.
[45] Lan, N.C., Ha, N.H., Tuan, N.A., Tuan, V.A., Dong, N.H., 2021. Static and cyclic properties of municipal solid bottom ash in Vietnam. Int J GEOMATE 20, 152–158.
[46] OECD Test No. 201: freshwater alga and cyanobacteria, growth inhibition test. OECD guidelines for the testing of chemicals, Section 2. OECD Editions. Paris. 2006.
[47] Geis, S.W., Fleming, K.L., Korthals, E.T., Searle, G., Reynolds, L., Karner, D.A., 2000. Modifications to the algal growth inhibition test for use as a regulatory assay. Environ Toxicol Chem 19, 36–41. https://doi.org/10.1897/1551-5028(2000)019<0036:mttagi>2.3.co;2.
[48] Stein, J.R., 1973. Handbook of Phycological Methods: Culture Methods and Growth Measurements. Cambridge University Press, Cambridge.
[49] OECD Test no. 221: Lemna sp. growth inhibition test. OECD guidelines for the testing of chemicals, Section 2. OECD editions. Paris. 2006.
[50] Kaza, M., Mankiewicz-Boczek, J., Izydorczyk, K., Sawicki, J., 2007. Toxicity assessment of water samples from rivers in central Poland using a battery of microbiotests - a pilot study. Pol J Environ Stud 16, 81–89.
[51] OECD Test no. 202: Daphnia sp. acute immobilisation test. OECD guidelines for the testing of chemicals, Section 2. OECD editions. Paris. 2004.
[52] ASTM Report E729–80, Standard Practice for Conducting Acute Toxicity Tests with Fishes, Macroinvertebrates and Amphibians. Materials; Philadelphia, PA, 1980;
[53] C.A. Schneider W.S. Rasband K.W. Eliceiri W.S. Rasband U.S. ImageJ National Institutes of Health, Bethesda, Maryland USA 2012 1997 2018.〈https://imagej.nih.gov/ij/〉.
[54] Azeiteiro, R.J.N., Coelho, P.A.L.F., Taborda, D.M.G., Grazina, J.C.D., 2017. Energy-based evaluation of liquefaction potential under non-uniform cyclic loading. Soil Dyn Earthq Eng 92, 650–665. https://doi.org/10.1016/j.soildyn.2016.11.005.
[55] Azeiteiro, R.J.N., Coelho, P.A.L.F., Taborda, D.M.G., Grazina, J.C.D., 2017. Critical state–based interpretation of the monotonic behavior of Hostun sand. J Geotechn Geoenviron Eng 143. https://doi.org/10.1061/(ASCE)GT.1943-5606.0001659.
[56] Kim, M., Seo, H., 2019. Evaluation of one - and two - parameter models for estimation of void ratio of binary sand mixtures deposited by dry pluviation. Granul Matter 21, 1–14. https://doi.org/10.1007/s10035-019-0925-3.
[57] Oyediran, I.A., Enya, N.I., 2021. Crude oil effects on some engineering properties of sandy alluvial soil. Int J Min Geo-Eng 55, 7–10. https://doi.org/10.22059/IJMGE.2020.283051.594815.
[58] Schaefer, V.R.; Berg, R.R.; Collin, J.G.; Christopher, B.R.; DiMaggio, J.A.; Filz, G. M.; Bruce, D.A.; Ayala, D.. Ground Modification Methods Reference Manual - Volume I. Publication No. FHWA-NHI-16–027. U.S. Dep. Transp. Fed. Highw. Adm. 2017.
[59] Duda, A., Siwowski, T.W., 2022. Stability and settlement analysis of a lightweight embankment filled with waste tyre bales over soft ground. Transp Infrastruct Geotechnol 9, 467–491. https://doi.org/10.1007/s40515-021-00184-5.
[60] Marradi, A., Pinori, U., Betti, G., 2012. The use of lightweight materials in road embankment construction. Procedia - Soc Behav Sci 53, 1001–1010. https://doi.org/10.1016/j.sbspro.2012.09.949.
[61] Humphrey, D.N., 2008. Tire derived aggregate as lightweight fill for embankments and retaining walls. In: Hazarika, H., Kazuya, Y. (Eds.), In Scrap Tire Derived Geomaterials - Opportunities and Challenges. Taylor & Francis, London, pp. 59–82.
[62] Ameratunga, J., Sivakugan, N., Das, B.M., 2016. Correlations of Soil and Rock Properties in Geotechnical Engineering. Springer, New Delhi.
[63] El-Deeb Ghazy, M.M., Habashy, M.M., Mohammady, E.Y., 2011. Effects of pH on survival, growth and reproduction rates of the crustacean, Daphnia magna. Aust J Basic Appl Sci 5, 1–10.
[64] Karna, R.R., Luxton, T., Bronstein, K.E., Hoponick Redmon, J., Scheckel, K.G., 2017. State of the science review: Potential for beneficial use of waste by-products for in situ remediation of metal-contaminated soil and sediment. Crit Rev Environ Sci Technol 47, 1–65. https://doi.org/10.1080/10643389.2016.1275417.
[65] Festa, R.A., Thiele, D.J., 2011. Copper: an essential metal in biology. Curr Biol 21, R877–R883. https://doi.org/10.1016/j.cub.2011.09.040.
[66] Astrup, T.; Muntoni, A.; Polettini, A.; Pomi, R.; Van Gerven, T.; Van Zomeren, A. Treatment and Reuse of Incineration Bottom Ash. In Environmental Materials and Waste: Resource Recovery and Pollution Prevention.; Prasad, M.N.V., Shih, K., Eds.; Elsevier, 2016; pp. 607–645 ISBN 9780128039069.
[67] Lidelow, S., Lagerkvist, A., 2007. Evaluation of leachate emissions from crushed rock and municipal solid waste incineration bottom ash used in road construction. Waste Manag 27, 1356–1365. https://doi.org/10.1016/j.wasman.2006.07.021.
[68] Cristelo, N., Segadães, L., Coelho, J., Chaves, B., Sousa, N.R., de Lurdes Lopes, M., 2020. Recycling municipal solid waste incineration slag and fly ash as precursors in low-range alkaline cements. Waste Manag 104, 60–73. https://doi.org/10.1016/j.wasman.2020.01.013.

[69] Chandler, A.J.; Eighmy, T.T.; Hartlén, J.; O..Hjelmar; Kosson, D.S.; Sawell, S.E.; Sloot, H.A. van der; Vehlow, J. Municipal Solid Waste Incinerator Residues. The International Ash Working Group (IAWG); Studies in Environmental Science, 67. Elsevier: Amsterdam, The Netherlands, 1997; ISBN 0444825630.
[70] Bunge, R., 2018. Recovery of metals from waste incineration bottom ash. In: Holm, O., Thome-Kozmiensky, E. (Eds.), Treatment and Utilisation of Waste Incineration Bottom Ash. UMTEC and VBSA, Neuruppin, Germany, pp. 63–143.
[71] Andreola, F., Barbieri, L., Hreglich, S., Lancellotti, I., Morselli, L., Passarini, F., Vassura, I., 2008. Reuse of incinerator bottom and fly ashes to obtain glassy materials. J Hazard Mater 153, 1270–1274. https://doi.org/10.1016/j.jhazmat.2007.09.103.
[72] Ashraf, M.S., Ghouleh, Z., Shao, Y., 2019. Production of eco-cement exclusively from municipal solid waste incineration residues. Resour Conserv Recycl 149, 332–342. https://doi.org/10.1016/j.resconrec.2019.06.018.
[73] Ginés, O., Chimenos, J.M., Vizcarro, A., Formosa, J., Rosell, J.R., 2009. Combined use of MSWI bottom ash and fly ash as aggregate in concrete formulation: Environmental and mechanical considerations. J Hazard Mater 169, 643–650. https://doi.org/10.1016/j.jhazmat.2009.03.141.
[74] Huber, F., Blasenbauer, D., Aschenbrenner, P., Fellner, J., 2019. Chemical composition and leachability of differently sized material fractions of municipal solid waste incineration bottom ash. Waste Manag 95, 593–603. https://doi.org/10.1016/j.wasman.2019.06.047.
[75] Monteiro, R.C.C., Figueiredo, C.F., Alendouro, M.S., Ferro, M.C., Davim, E.J.R., Fernandes, M.H.V., 2008. Characterization of MSWI bottom ashes towards utilization as glass raw material. Waste Manag 28, 1119–1125. https://doi.org/10.1016/j.wasman.2007.05.004.
[76] Neuwahl, F.; Cusano, G.; Benavides, J.G.; Holbrook, S.; Serge, R. Best Available Techniques (BAT) Reference Document for Waste Incineration. Industrial Emissions Directive 2010/75/EU (Integrated Pollution Prevention); Science for Policy report by the Joint Research Centre, European Commission, Luxembourg, 2019;
[77] Rambaldi, E., Esposito, L., Andreola, F., Barbieri, L., Lancellotti, I., Vassura, I., 2010. The recycling of MSWI bottom ash in silicate based ceramic. Ceram Int 36, 2469–2476. https://doi.org/10.1016/j.ceramint.2010.08.005.
[78] Rendek, E., Ducom, G., Germain, P., 2007. Influence of waste input and combustion technology on MSWI bottom ash quality. Waste Manag 27, 1403–1407. https://doi.org/10.1016/j.wasman.2007.03.016.
[79] Tang, P., Florea, M.V.A., Spiesz, P., Brouwers, H.J.H., 2015. Characteristics and application potential of municipal solid waste incineration (MSWI) bottom ashes from two waste-to-energy plants. Constr Build Mater 83, 77–94. https://doi.org/10.1016/j.conbuildmat.2015.02.033.
[80] Zhang, Z., Zhang, L., Li, A., 2015. Development of a sintering process for recycling oil shale fly ash and municipal solid waste incineration bottom ash into glass ceramic composite. Waste Manag 38, 185–193. https://doi.org/10.1016/j.wasman.2014.12.028.
[81] Bayuseno, A.P., Schmahl, W.W., 2010. Understanding the chemical and mineralogical properties of the inorganic portion of MSWI bottom ash. Waste Manag 30, 1509–1520. https://doi.org/10.1016/j.wasman.2010.03.010.
[82] Hyks, J., Astrup, T., Christensen, T.H., 2009. Leaching from MSWI bottom ash: evaluation of non-equilibrium in column percolation experiments. Waste Manag 29, 522–529. https://doi.org/10.1016/j.wasman.2008.06.011.
[83] Lindberg, D., Molin, C., Hupa, M., 2015. Thermal treatment of solid residues from WtE units: a review. Waste Manag 37, 82–94. https://doi.org/10.1016/j.wasman.2014.12.009.
[84] Klymko, T., Dijkstra, J.J., van Zomeren, A., 2017. Guidance document on hazard classification of MSWI bottom ash. ECN Rep; Petten, Neth.
[85] Chimenos, J.M., Fernández, A.I., Nadal, R., Espiell, F., 2000. Short-term natural weathering of MSWI bottom ash. J Hazard Mater 79, 287–299. https://doi.org/10.1016/S0304-3894(00)00270-3.
[86] Maria, I.; Enric, V.; Xavier, Q.; Barra, M.; López, A.; Plana, F. Use of bottom ash from municipal solid waste incineration as a road material. In Proceedings of the International Ash Utilization Symposium, Center for Applied Energy Research, University of Kentucky; 2001.
[87] LNEC, 2015. Laboratório Nacional de Engenharia Civil. Documento de aplicação. AEIRU - Agregados artificiais de escórias de incineração de resíduos urbanos para pavimentos rodoviários; Lisbon, Portugal.
[88] del Valle-zermeño, R., Chimenos, J.M., Giró-paloma, J., Formosa, J., 2014. Use of weathered and fresh bottom ash mix layers as a subbase in road constructions: environmental behavior enhancement by means of a retaining barrier. Chemosphere 117, 402–409. https://doi.org/10.1016/j.chemosphere.2014.07.095.
[89] Di, M., Hyks, J., Verginelli, I., Costa, G., Hjelmar, O., Lombardi, F., 2018. Leaching behaviour of incineration bottom ash in a reuse scenario: 12 years-field data vs. lab test results. Waste Manag 73, 367–380. https://doi.org/10.1016/j.wasman.2017.08.013.
[90] Gao, B., 2012. Phosphorus Recovery from Sorted MSWI Bottom Ash: the Acidic Dissolution – Precipitation Method. Chalmers University of Technology, Göteborg, Sweden.
[91] Loginova, E., Volkov, D.S., van de Wouw, P.M.F., Florea, M.V.A., Brouwers, H.J.H., 2019. Detailed characterization of particle size fractions of municipal solid waste incineration bottom ash. J Clean Prod 207, 866–874. https://doi.org/10.1016/j.jclepro.2018.10.022.
[92] Chen, B.; Brito van Zijl, M.; Keulen, A.; Ye, G. Thermal Treatment on MSWI Bottom Ash for the Utilisation in Alkali Activated Materials. In Proceedings of the RICON19 - REMINE International Conference on Valorization of mining and industrial wastes into construction materials by alkali-activation; 2020; pp. 25–35.
[93] Šyc, M., Simon, F.G., Hykš, J., Braga, R., Biganzoli, L., Costa, G., Funari, V., Grosso, M., 2020. Metal recovery from incineration bottom ash: State-of-the-art and recent developments. J Hazard Mater 393, 122433. https://doi.org/10.1016/j.jhazmat.2020.122433.
[94] Faleschini, F., Toska, K., Zanini, M.A., Andreose, F., Settimi, A.G., Brunelli, K., Pellegrino, C., 2021. Assessment of a municipal solid waste incinerator bottom ash as a candidate pozzolanic material: comparison of test methods. Sustainability 13, 8998. https://doi.org/10.3390/su13168998.
[95] Cheeseman, C.R., Monteiro Da Rocha, S., Sollars, C., Bethanis, S., Boccaccini, A. R., 2003. Ceramic processing of incinerator bottom ash. Waste Manag 23, 907–916. https://doi.org/10.1016/S0956-053X(03)00039-4.
[96] Onori, R. Alkaline activation of incinerator bottom ash for use in structural applications., Sapienza University of Rome, 2011.
[97] Pöykiö, R., Manskinen, K., Nurmesniemi, H., Dahl, O., 2011. Comparison of trace elements in bottom ash and fly ash from a large-sized (77 MW) multi-fuel boiler at the power plant of a fluting board mill, Finland. Energy Explor Exploit 29, 217–233.
[98] Suescum-Morales, D., Silva, R.V., Bravo, M., Jiménez, J.R., Fernández-Rodríguez, J.M., de Brito, J., 2022. Effect of incorporating municipal solid waste incinerated bottom ash in alkali-activated fly ash concrete subjected to accelerated CO_2 curing. J Clean Prod 370, 133533. https://doi.org/10.1016/j.jclepro.2022.133533.
[99] Mantovani, L., Tribaudino, M., De Matteis, C., Funari, V., 2021. Particle size and potential toxic element speciation in municipal solid waste incineration (Mswi) bottom ash. Sustainability 13, 1911. https://doi.org/10.3390/su13041911.
[100] Almeida, F., Carneiro, J.R., Lopes, M., de, L., 2020. Use of incinerator bottom ash as a recycled aggregate in contact with nonwoven geotextiles: Evaluation of mechanical damage upon installation. Sustainability 12, 9156. https://doi.org/10.3390/su12219156.
[101] Fulladosa, E., Murat, J.C., Martínez, M., Villaescusa, I., 2005. Patterns of metals and arsenic poisoning in Vibrio fischeri bacteria, 60, 43–48. https://doi.org/10.1016/j.chemosphere.2004.12.026.
[102] Stiernström, S., Hemström, K., Wik, O., Carlsson, G., Bengtsson, B.E., Breitholtz, M., 2011. An ecotoxicological approach for hazard identification of energy ash. Waste Manag 31, 342–352. https://doi.org/10.1016/j.wasman.2010.05.019.
[103] Zamani, M., Badv, K., 2019. Assessment of the geotechnical behavior of collapsible soils: a case study of the mohammad-abad railway station soil in semnan. Geotech Geol Eng 37, 2847–2860. https://doi.org/10.1007/s10706-018-00800-1.
[104] Lins, Y.; Schanz, T. Determination of hydro-mechanical Properties of Sand. In Unsaturated soils: experimental studies.; Schanz, T., Ed.; Springer: Berlim, Germany, 2003; pp. 15–32 ISBN 3540211217.
[105] Mesri, G., Vardhanabhuti, B., 2009. Compression of granular materials. Can Geotech J 369–392.
[106] Zheng, J., Hryciw, R.D., Ventola, A., 2017. Compressibility of sands of various geologic origins at pre-crushing stress levels. Geotech Geol Eng 35, 2037–2051. https://doi.org/10.1007/s10706-017-0225-9.
[107] Regmi, N.R., Giardino, J.R., McDonald, E.V., Vitek, J.D., 2015. A review of mass movement processes and risk in the critical zone of Earth. Dev Earth Surf Process 19, 319–362.
[108] Terzaghi, K., Peck, R.B., 1967. Soil Mechanics in Engineering Practice. John Wiley. John Wiley & Sons, New York, USA.